DOI: 10.1534/genetics.106.069575

A Maternal Screen for Genes Regulating Drosophila Oocyte Polarity Uncovers New Steps in Meiotic Progression

Vitor Barbosa, Naomi Kimm and Ruth Lehmann[1]

Howard Hughes Medical Institute and the Kimmel Center for Biology and Medicine of the Skirball Institute, New York, New York 10016 and Development Genetics Program, New York University Medical Center, New York, New York 10016

Manuscript received December 26, 2006
Accepted for publication April 23, 2007

ABSTRACT

Meiotic checkpoints monitor chromosome status to ensure correct homologous recombination, genomic integrity, and chromosome segregation. In Drosophila, the persistent presence of double-strand DNA breaks (DSB) activates the ATR/Mei-41 checkpoint, delays progression through meiosis, and causes defects in DNA condensation of the oocyte nucleus, the karyosome. Checkpoint activation has also been linked to decreased levels of the TGFα-like molecule Gurken, which controls normal eggshell patterning. We used this easy-to-score eggshell phenotype in a germ-line mosaic screen in Drosophila to identify new genes affecting meiotic progression, DNA condensation, and Gurken signaling. One hundred eighteen new ventralizing mutants on the second chromosome fell into 17 complementation groups. Here we describe the analysis of 8 complementation groups, including Kinesin heavy chain, the SR protein kinase *cuaba*, the cohesin-related gene *dPds5/cohiba*, and the Tudor-domain gene *montecristo*. Our findings challenge the hypothesis that checkpoint activation upon persistent DSBs is exclusively mediated by ATR/Mei-41 kinase and instead reveal a more complex network of interactions that link DSB formation, checkpoint activation, meiotic delay, DNA condensation, and Gurken protein synthesis.

As cells divide, checkpoints delay the transition to the next phase of each cycle until the previous phase is completed to ensure the genomic stability of the daughter cells (Kuzminov 2001). During meiosis in yeast, this surveillance allows the correct reduction of the DNA content into fully functional gametes (Roeder and Bailis 2000). Similarly, in Drosophila, the activation of a meiotic checkpoint is thought to delay meiotic progression in the oocyte (Huynh and St Johnston 2000).

Drosophila oogenesis begins at the anterior tip of the germarium, as cystoblasts divide synchronously to form cysts of 16 interconnected germ cells (Figure 1) (Spradling 1993; de Cuevas *et al.* 1997). Several cells in each cyst enter meiotic prophase, condense their chromosomes, form synapses between the homologs, and repair double-strand breaks (DSB) in the DNA, but only one cystocyte reaches the full pachytene state (Carpenter 1979; Page and Hawley 2001, 2004; Jang *et al.* 2003). Mutations in meiotic genes, such as the DSB repair genes *okra/dRad54* (*okr*) and *spindle-A/dRad51* (*spn-A*), delay this restriction. In later stages, DSB repair mutants show fragmented or thread-like chromatin organization within the oocyte nucleus instead of condensing into a hollow spherical "karyosome" as in the wild type (Gonzalez-Reyes *et al.* 1997; Huynh and St Johnston 2000; Staeva-Vieira *et al.* 2003).

In addition to delays in meiotic restriction, females with mutant DSB repair enzymes lay eggs with dorsal–ventral (DV) defects known as the *spindle* phenotype (Gonzalez-Reyes *et al.* 1997; Ghabrial *et al.* 1998; Morris and Lehmann 1999; Staeva-Vieira *et al.* 2003). The persistence of DSBs in these mutants activates the ATR-like kinase Mei-41 and the Drosophila checkpoint protein 2 (dChk2) (Ghabrial and Schupbach 1999; Abdu *et al.* 2002; Staeva-Vieira *et al.* 2003). This activation causes modification of Vasa (Vas), a germline-specific ATP-dependent helicase required for translation of a number of mRNAs, including that of the TGFα-like molecule *gurken* (*grk*) (Neuman-Silberberg and Schupbach 1994; Styhler *et al.* 1998; Ghabrial and Schupbach 1999). Grk is required during mid-oogenesis to establish the DV axis of the future eggshell (Ghiglione *et al.* 2002). Therefore, the activation of the Mei-41 checkpoint can prevent oocyte development.

Little is known about the effectors of the meiotic checkpoint that lead to delays in meiotic progression or oocyte polarity defects. Previous genetic screens based on female sterility and the *spindle* phenotype also identified DV polarity genes with functions other than DSB repair (Schupbach and Wieschaus 1989, 1991; Morris *et al.* 2003; Staeva-Vieira *et al.* 2003). These included genes required for *grk* mRNA transport (Swan and Suter 1996; Swan *et al.* 1999; Brendza *et al.* 2000;

[1]*Corresponding author:* Development Genetics Program, Skirball Institute, NYU Medical Center, 540 First Ave., New York, NY 10016. E-mail: lehmann@saturn.med.nyu.edu

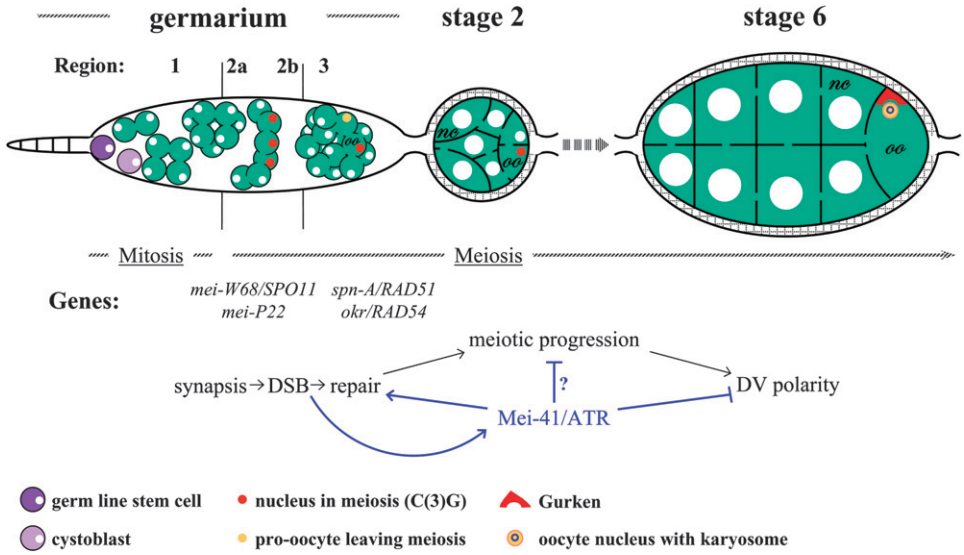

FIGURE 1.—Schematic of the onset of Drosophila female meiosis. The germarium is the most anterior structure of the Drosophila ovariole, where germ-line stem cells produce cystoblasts by asymmetric division. Germaria are divided into three regions. In region 1, cystoblast formation is followed by four rounds of mitosis, which give rise to cysts of 16 interconnected cells. In region 2, several cells per cyst initiate the assembly of synaptic chromosomes and form DSBs through the activity of the Drosophila *SPO11* homologs *mei-W68* and *mei-P22*. In region 3A, cysts become surrounded by follicle cells (not shown) and reorient so that each oocyte is placed at the posterior pole of each cluster where it remains for the rest of oogenesis. At stage 2, meiotic restriction to the oocyte (*oo*) is completed. The other "synaptic" cystocytes regress from meiosis and become nurse cells (*nc*). As the oocyte leaves pachytene, the meiotic chromatin releases the synaptonemal complex components and condenses into a karyosome (blue doughnut). In mid-oogenesis, the oocyte nucleus moves anteriorly. Tightly associated with it, Grk will be secreted to the adjacent follicle cells (gray grid), which will acquire a dorsal fate and later synthesize the dorsal appendages of the chorion (not shown). Persistent DSB in *spn-A* and *okr* mutants activate Mei-41, which causes a decrease in Grk production and consequent ventralization of the eggshell. The link between this activation and delays in meiotic progression is unclear (blue question mark).

HUYNH and ST JOHNSTON 2000; NAVARRO *et al.* 2004; ABDU *et al.* 2006), genes required for Grk processing (STYHLER *et al.* 1998; MIURA *et al.* 2006), and genes regulating the stability and trafficking of Grk protein (SAUNDERS and COHEN 1999; KENNERDELL *et al.* 2002; FINDLEY *et al.* 2003; WILHELM *et al.* 2005; BOKEL *et al.* 2006).

In addition to DNA repair, different checkpoint pathways may monitor other meiotic steps (BHALLA and DERNBURG 2005). Here we describe a large-scale mutagenesis screen to isolate mutations in genes linking the control of meiotic progression with oocyte development. Using Grk expression in the oocyte, oocyte nuclear markers, and genetic analysis, we characterize eight loci and group them into phenotypic classes according to their effect on meiotic chromatin condensation, DSB formation, meiotic checkpoint pathway activation, and DV polarity. Among DSB repair candidate genes, we identify the Drosophila cohesin-related gene *dPds5* and the novel Tudor-domain gene *montecristo* (*mtc*). The characterization of their phenotypes provides evidence that additional mechanisms independent of the meiotic checkpoint kinase, Mei-41, delay meiosis and affect oocyte polarity. Two other mutants, *indios* (*nds*) and *trinidad* (*trin*), suggest the possibility that the process of meiotic chromatin condensation can be uncoupled from the Grk-mediated signaling pathway.

MATERIALS AND METHODS

Fly stocks: The following alleles identified in the screen were used for phenotypic analysis: khc^{bgs1}, khc^{bgs2}, eight $dPds5^{cohiba}$ alleles (1–8), blv^{1}, blv^{2}, nds^{2}, nds^{4}, $trin^{1}$, $trin^{3}$, three *mtc* alleles (1–3), three $srpk^{cuaba}$ alleles (1–3), and bha^{1} and bha^{2}. $mei\text{-}41^{D3}$, $mei\text{-}W68^{1}$, $mei\text{-}P22^{1}$, $spn\text{-}A^{1}$, $spn\text{-}A^{093A}$, okr^{RU}, and okr^{AA} were present in the laboratory. khc^{27}, *P{lacW}l(2)k1223*, *PBac{WH}CG15707*^{f06583}, the 2R deficiencies, and all the starting lines used in the screen (see below) were obtained from Bloomington Stock Center. All flies were raised at 25° unless otherwise indicated.

Mutagenesis: The screen was carried out as previously described for the 3R chromosome (YOHN *et al.* 2003). Males of the genotype *w P{w*$^{+}$ *faf-LacZ}*; *P{w*$^{+}$ FRT 42B*}* were starved and treated with 25 or 35 mM ethylmethane sulfonate (EMS) (Sigma, St. Louis) in 1% sucrose for 16–24 hr as described (ASHBURNER 1989). Lac-Z expression from the *P{w*$^{+}$ *faf-LacZ}* transgene localizes to the pole plasm and persists in the primordial germ cells throughout embryogenesis. *P{w*$^{+}$ FRT 42B*}* carries the FRT sequence in region 42B of a recently isogenized second chromosome. Mutagenized males were crossed to females of the genotype *w P{w*$^{+}$ *faf-LacZ}*; *If/*CyO *hs-hid*, in which CyO *hs-hid* is a balancer CyO bearing the heat-shock-inducible proapoptotic transgene *head involution defective* (*hid*). This cross was set up in bottles and flipped daily to fresh food four times, after which males were discarded. Twenty thousand single virgin females carrying a mutagenized *P{w*$^{+}$ FRT 42B*}* chromosome in *trans* to CyO *hs-hid* were crossed to males of the genotype *y w P{ry*$^{+}$ *hs-FLP*^{22}*}*/Y; *P{w*$^{+}$ FRT 42B*} P{w*$^{+}$ *ovo*^{D}*}*/CyO *hs-hid* (see Figure 2A for a schematic of the screen). The *P{ry*$^{+}$ *hs-FLP*^{22}*}* transgene allows the production of the yeast FRT-specific recombinase FLP, whereas *P{w*$^{+}$ *ovo*^{D}*}* inserts the dominant female sterile ovo^{D} allele in the FRT42B chromosome (CHOU and PERRIMON 1992). On the fifth or sixth day after mating, the parents were discarded and the F_1 larvae were heat-shocked in a 37° water bath for 2 hr to induce mitotic recombination and death of individuals carrying the balancer. F_1 adults were transferred to fresh yeasted food for 3 days before egg collection. Eggs derived from germ-line clones were collected twice. The first collection was stained for β-galactosidase activity to visualize

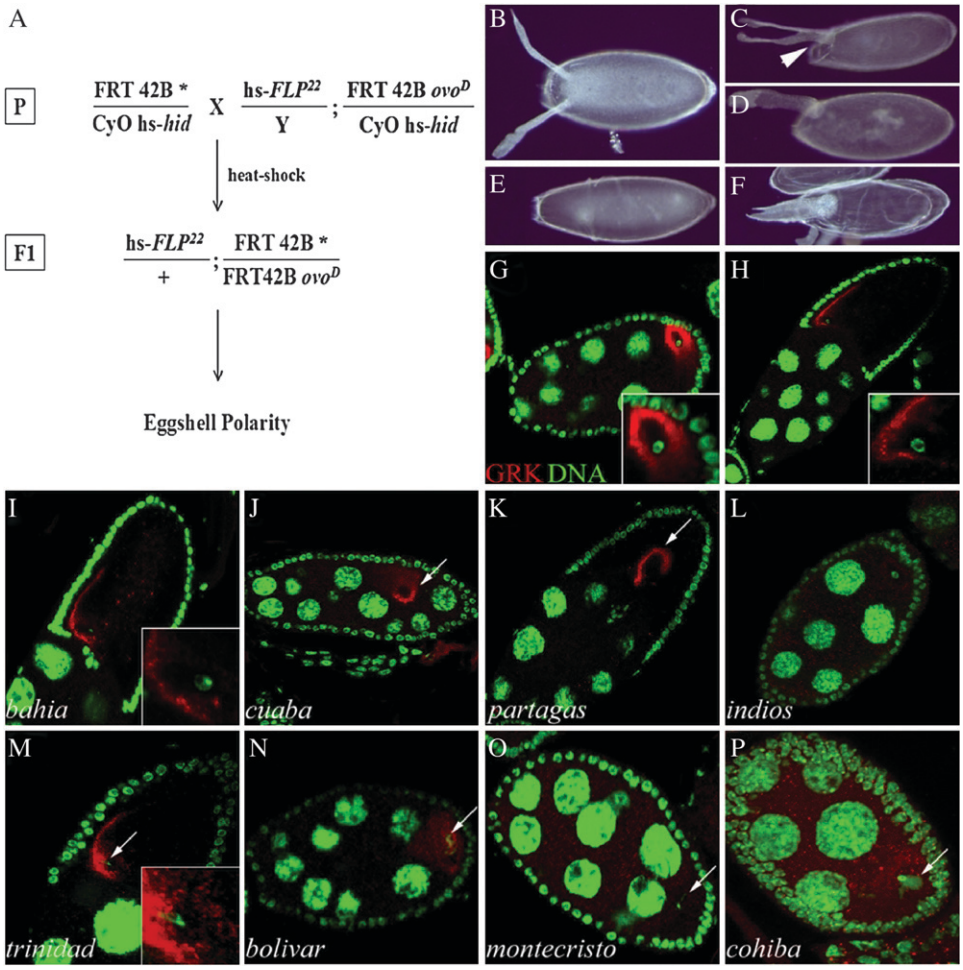

FIGURE 2.—Karyosome and Grk phenotypes in DV polarity mutant egg chambers. (A) Schematic of the clonal screen procedure. Each parental (P) female carried one mutagenized second chromosome with the FRT sequence proximally inserted in its right arm (FRT 42B*). Virgins were crossed to males carrying a second chromosome with the same FRT insertion and the dominant female sterile *ovo* allele (FRT42B ovo^D). Heat-shock-induced mitotic recombination in the germ line ($hs\text{-}FLP^{22}$) and death of balanced (CyO *hs-hid*) F_1 larvae. Eggshell polarity defects in the resulting eggs were identified and stocks established (MATERIALS AND METHODS). (B–F) Ventralization of the eggshell. (B) Wild-type egg from a $dPds5^{cohiba}$/CyO control fly. (C) Mildly ventralized eggshell from a nds^2/nds^4 fly with DAs fused at the base (arrowhead). (D) Ventralized egg showing a single DA from a bha^1/bha^2 fly. (E) Extreme ventralization with absent DAs and elongated eggshell from $dPds5^1$ homozygous germ-line clone. (F) Example of a small/collapsed mutation derived from a $srpk^2/srpk^4$ heterozygous fly. (G–P) Localization of Grk (red) and DNA (green) in oogenesis. (G–H) Wild-type stages 6 (G) and 10 (H) egg chambers and higher magnifications of each oocyte nucleus (insets) from *mtc*/CyO flies. (I–K) Class I mutants showing normal karyosome morphology and Grk levels. (I) Stage 10 bha^1/bha^2 egg chamber. (J) Stage 6 chamber homozygous for $srpk^2$ showing a misplaced oocyte (arrow). (K) khc^{pgs1} mutant stage 10 with arrow pointing to the oocyte nucleus, which is associated with Grk but is not anchored to the anterior cortex. (L) Class II nds^2/nds^4 stage 6 chamber showing decreased levels of Grk and normal karyosome. (M) Class III, $trin^1/trin^2$ stage 10 chamber with normal Grk but collapsed karyosome (arrow and inset). (N–P) Class IV mutations showing decreased Grk levels. (N) A blv^1/blv^3 stage 6/7 chamber showing a typical thread-like karyosome defect (arrow). (O) A stage 6 mtc^2/mtc^3 egg chamber with a similar karyosome defect (arrow). (P) Stage 6 $dPds^2$ homozygous germ-line clone. The oocyte nucleus (arrow) shows a region of expanded chromatin apparently emanating from a more condensed core.

germplasm and germ cells by virtue of the *P{w⁺faf-LacZ}* transgene (MOORE *et al.* 1998). This was used to detect defects in germ cell formation or migration (data not shown). The second collection was screened directly on the egg deposition plate for eggshell phenotypes (STAEVA-VIEIRA *et al.* 2003). The lines of interest were established by crossing F_1 *w P{w⁺faf-LacZ}/Y; P{w⁺* FRT 42B*}*/P{w⁺* FRT 42B*} P{w⁺ ovoᴰ}* males to females of the genotype *w P{w⁺faf-LacZ}; Sp P{w⁺ hs-hid}*/CyO, *P{ry⁺faf-LacZ}* and heat-shocking the F_2 larvae. To generate stable lines, single F_2 *Cy* males were crossed back to *w P{w⁺faf-LacZ}; Sp P{w⁺ hs-hid}*/CyO, *P{ry⁺faf-LacZ}* females and the progeny heat-shocked as larvae. Only the F_2 males carrying the *P{w⁺* FRT 42B*}** chromosome would produce viable offspring.

Germ-line clones homozygous for 310 mutations causing DV defects were rescreened. Lines producing wild-type eggshells (18 lines) were discarded as false positives. Mutations causing defects in the eggshell without affecting its DV patterning (174 lines) were sent to L. Cooley (Yale University). The penetrance of the DV phenotype of the remaining 118 lines was quantified in this secondary screen as frequency of ventralized eggshells ($n > 300$). Mutant lines were divided into "strong" (from 80 to 100% ventralized eggshells), "medium" (from 50 to 70% of ventralized eggshells), "weak" (~30% ventralization), and "small/collapsed" (in addition to ventralized, eggshells were small and/or collapsed, Figure 2F) categories.

Complementation testing and deficiency mapping: Mutants of the strong, medium, and small/collapsed categories were used in complementation crosses (Table 2). The criteria for lack of complementation were lethality or >30% ventralized eggshells. With these criteria, three lines failed to complement more than one complementation group, indicating the presence of double mutants $srpk^{cuaba4}$ and $veguero^3$, $corona^2$ and $fonseca^2$, and $troya^2$ and $vegueiro^1$.

Lethal complementation groups were directly mapped using the Bloomington 2R deficiency kit. Each deficiency failing to complement lethality was then confirmed by crossing it with all the other mutants in the same complementation group. Deficiencies of the kit were also used to confirm the mapping of viable complementation groups after rough SNP mapping (see below). Complementation tests with known mutations mapped in each region were also performed for $khc^{partagas}$, $srpk^{cuaba}$, $dPds5^{cohiba}$, *mtc*, and *blv*.

TABLE 1

SNPs defining a rough molecular map of 2R

Primer name[a]	Primer sequence[b]	Cytologic region[c]	Enzyme used
pnut 4 L	GCGGCATGAGGGATGCTGAA	44C1	*Cla*I
pnut 4 R	TGCGCGAAAATTCCAACCGA		
egr 8 L	CGGCTTTGCCTCGCTTCGTT	46F4	*Ava*I
egr 8 R	CGGTGGCAGATTCGTCCTGCT		
jeb 2 L	CGGGAAAGGGGAGGACGCAG	48E2	*Pvu*II
jeb 2 R	TATTGGGGGCGGCGAAAGGT		
mam 4L	ACGCTGCCGCCTCTGTTGCT	50D1	*Alu*II
mam 4R	CGCCCTCCCGCTCTGCATTT		
Flo 4 L	GCACGGGTTGATTGACCGGAA	52B1	*Hha*I
Flo 4 R	CTTGTCCGCCGCTCCCCTCT		
rhi 3 L	CGTGTGTGAAGGGGAAGGGCA	54D3	*Mwo*I
rhi 3 R	GCTTCGGTGCTCATTGCGG		
hts 4 L	CGGTCGGGTCGAAAGCGAGA	56D8	*Taq*I
hts 4 R	CGCTGGTGGCTGTGTGTATGCC		
clt 3 L	GCACGTCCATCCGCCAAGTGA	57F2	*Rsa*I
clt 3 R	TGCCACTCAGCTCCCCAGCA		
bw 1 L	GCCTCCATCGGCGTTTCGCT	59D11	*Bsa*JI
bw 1 R	TGTGAGGGGGTGTGGTGGGG		

[a] Primers and SNPs were named after known 2R genes molecularly mapped to each interval. pnut, *peanut*; egr, *eiger*; jeb, *jelly belly*; mam, *mastermind*; Flo, *Flotillin*; rhi, *rhino*; hts, *hu li tai shao*; clt, *cricklet*; and bw, *brown*.

[b] 5′–3′ sequence.

[c] Region containing the SNP–RFLP.

Genetic mapping with single nucleotide polymorphism markers: Nonessential loci were mapped to an approximate resolution of 2 Mb, similar to assays previously described (Berger *et al.* 2001). Single nucleotide polymorphisms (SNPs) causing restriction fragment-length polymorphism (RFLP) defining 10 evenly spaced intervals along 2R were selected (Table 1). The SNPs were defined between the *P{w*$^+$ FRT 42B*}* chromosome (used for mutagenesis) and a divergent isogenized chromosome containing the distal marker *If* (used to generate recombinants for mapping). The SNP map was constructed by a light shotgun sequencing approach (Berger *et al.* 2001). Primers were designed to PCR amplify nine genomic fragments of ~1 kb along both chromosomes (Table 1). The sequence of each FRT 42B PCR product was then compared to the *If* chromosome using SeqMan and MapDraw software (DNASTAR, Madison, WI) to find SNPs affecting the restriction site of common endonucleases (Table 1). These sites were tested by digesting PCR products generated from 10 single fly genomic DNA preparations of the genotypes *P{w*$^+$ FRT 42B*}/P{w*$^+$ FRT 42B*}* and *P{w*$^+$ FRT 42B*}/If* as well as from genomic DNA isolated from *If/If* embryos. All enzymes were commercially available (NEB, Ipswich, MA).

The mapping cross was as follows: *w*; *If/P{w*$^+$ FRT 42B*} m*^{1} females crossed to *w*/Y; *P{*Δ*w* FRT 42B*} m*^{2}/CyO males, where *m*^{1} and *m*^{2} represent any two alleles of the complementation group *m*. *P{*Δ*w* FRT 42B*}* was derived from a *P{w*$^+$ FRT 42B*}* chromosome from which the *w*$^+$ marker was removed by intramolecular recombination leaving the intact FRT sequence on the chromosome. Recombination events on 2R were recovered over *P{*Δ*w* FRT 42B*} m*^{2} in the following generation and identified by their nonparental phenotypes: *w If*$^+$ *Cy*$^+$ and *w*$^+$ *If Cy*$^+$. Combined with the eggshell phenotype of each single recombinant female, the SNP analysis allowed the linkage of each locus to 1 of 10 intervals defined by the centromere proximal *w*$^+$ transgene of the FRT42B insertion, the nine SNPs, and the centromere distal *If* (Tables 1 and 2).

Allele sequencing and molecular cloning: Preparation of genomic DNA and sequencing reactions were carried out as described (Staeva-Vieira *et al.* 2003). Each mutant sequence from *P{w*$^+$ FRT 42B*} m*/Df(2R) was aligned with that of the homozygous *P{w*$^+$ FRT 42B*}* chromosome using DNASTAR.

To molecularly map the *P{lacW}l(2)k1223* insertion, inverse PCR was carried out according to the Berkeley Drosophila Genome Project Resources website but using only the *Sau*3AI restriction enzyme. Sequences in the 3′ and 5′ ends of the *P* element obtained from two independent trials were compared with the Drosophila genome release 3, and the adjacent coding region *CG17509* was sequenced in *P{w*$^+$ FRT 42B*} dPds5*^{cohiba}/Df(2R) mutants as above.

Immunostaining Drosophila ovaries: Ovaries were processed for immunofluorescence as described (Navarro *et al.* 2004). The monoclonal anti-Grk antibody 1D12 (Developmental Studies Hybridoma Bank) and the rabbit polyclonal anti-C(3)G antibody were diluted 1:50 and 1:1000, respectively (Queenan *et al.* 1999; Navarro *et al.* 2004). Cy3-conjugated (Jackson Immunoresearch, West Grove, PA) and Alexa 488-conjugated (Molecular Probes, Eugene, OR) secondary antibodies were used at a dilution of 1:500. DNA was stained with either Oligreen or DAPI (Molecular Probes) diluted 1:5000 and 0.3 μM, respectively, according to the company's instructions. Ovaries were mounted in Vectashield (Vector Labs, Burlingame, CA) and visualized with a Leica TCS NT confocal microscope (Leica, Bannockburn, IL).

For visualization of mutant germ-line clones, 2- or 3-day-old adult females of the genotype *y w P{ry*$^+$ *hs-FLP*^{22}*}*; *P{w*$^+$ FRT 42B*} P{w*$^+$ FRT *nls-GFP}*/CyO *hs-hid* were heat-shocked on two consecutive days for 1 hr each. Heat-shocked adults were transferred to fresh food for five additional days, fattened on fresh yeast on the sixth day, and dissected on the seventh day as described. The autofluorescence of nuclear GFP was always preferred to its indirect immunolabeling using commercially available antibodies.

TABLE 2

2R complementation groups isolated in the screen

Locus name	Allele no. and categories[a] s	m	w	c	Lethality[b]	Map[c]	Gene
partagas (*pgs*)	3	1	—	—	L	53A2	*CG7765*, *khc*
bahia (*bha*)	—	2	—	—	V	48E-50F	
cuaba	—	2	—	2	SL	51F11-12	*CG8174*, *srpk*
indios (*nds*)	3	1	—	—	V	57D2-58D1	
trinidad (*trin*)	2	4	—	1	V	52B1-54D2	
cohiba	4	4	—	—	L	48D7-8	*CG17509*, *dPds5*
montecristo (*mtc*)	—	2	—	1	V	53A1	*CG15707*, Tudor domain
bolivar (*blv*)	1	3	—	—	SL	59D11-60A7	
troya	1	6	—	—	L	51D3-52F9	
diplomatico	—	1	—	1	L		
sancho panza	—	1	—	1	V		
romeo y julieta	—	1	—	1	V		
guantanamera	—	—	—	2	L		
corona	—	—	—	2	V		
veguero	—	2	—	1	L		
rey del mundo	—	2	—	—	L		
fonseca	1	—	—	1	L		
Single alleles	3	17	31	10	—		

[a] Categories are based on frequency of ventralized eggshells (see MATERIALS AND METHODS). $n > 300$.
[b] Viability of transheterozygous adults. L, lethal; SL, semilethal or lower than expected number of adults; V, viable.
[c] Minimal cytological interval containing each gene.

Genetic interactions: The DV phenotype in viable or semilethal complementation groups was tested in a *mei-41* mutant background by comparing the frequency of ventralized eggshells in *mei-41^{D3}/mei-41^{D3}*; *P{w$^+$* FRT 42B*} m^1/P{w$^+$* FRT 42B*} m^2* and *mei-41^{D3}/FM7*; *P{w$^+$* FRT 42B*} m^1/P{w$^+$* FRT 42B*} m^2* flies. To assess genetic interactions with mutants defective in DSB (*mei-P22*), the frequency between *P{w$^+$* FRT 42B*} m^1/P{w$^+$* FRT 42B*} m^2*; *mei-P22^1/mei-P22^1* and *P{w$^+$* FRT 42B*} m^1/P{w$^+$* FRT 42B*} m^2*; *mei-P22^1*/TM3 flies was compared. For the alleles of each locus used in this study, see supplemental Table 1 (http://www.genetics.org/supplemental/). Interactions with lethal groups and the checkpoint were tested by heat-shock induction of germ-line clones in *mei-41^{D3}/mei-41^{D3}*; *P{w$^+$* FRT 42B*} l(2R)/P{w$^+$* FRT 42B*} P{w$^+$ ovo^D}*; MKRS *P{ry$^+$ hs-FLP^{22}}* and in *mei-41^{D3}/FM7*; *P{w$^+$* FRT 42B*} l(2R)/P{w$^+$* FRT 42B*} P{w$^+$ ovo^D}*; MKRS *P{ry$^+$ hs-FLP^{22}}* flies. *l(2R)* is any allele of the lethal groups tested, *khc^{pgs}* and *dPds5^{cohiba}*. *dPds5* mutants were tested in a DSB-free background by inducing germ-line clones in *y w P{ry$^+$ hs-FLP^{22}}*; *mei-41^{D3}/mei-41^{D3}*; *P{w$^+$* FRT 42B*} dPds5^{cohiba}/P{w$^+$* FRT 42B*} P{w$^+$ ovo^D}* and in *y w P{ry$^+$ hs-FLP^{22}}*; *mei-41^{D3}*/FM7; *P{w$^+$* FRT 42B*} dPds5^{cohiba}/P{w$^+$* FRT 42B*} P{w$^+$ ovo^D}*. As a positive control for each type of suppression, the allelic pair *okr^{RU}/okr^{AA}* was used except for the *dPds5, mei-W68* interaction experiments, for which *spn-A^1/spn-A^{093A}* was used (GHABRIAL *et al.* 1998; STAEVA-VIEIRA *et al.* 2003).

RESULTS

A screen for genes controlling meiosis and oocyte patterning: The Grk-mediated EGF receptor pathway is a sensitive readout for two fundamental processes of early oogenesis: meiosis and oocyte polarity. Abrogation of this pathway causes a characteristic ventralized eggshell phenotype that can be easily recognized by fusion or lack of the two dorsal appendages in the eggs of mutant females (Figure 2, B–F). We used this phenotype to identify new germ-line-specific genes on the right arm of chromosome 2 (2R) involved in meiotic progression and Grk ligand production. To isolate both lethal and viable EMS-derived mutations, we employed the FRT/*ovo^D* technique to produce germ-line clones homozygous for 2R in an otherwise heterozygous adult (Figure 2A) (CHOU and PERRIMON 1992). Among 8179 independent lines, we isolated 310 potential mutations, of which 118 were kept for further analysis after a secondary screen (MATERIALS AND METHODS).

The final 118 lines were divided into four categories—strong (18 lines), medium (47 lines), weak (31 lines), and small/collapsed (22 lines)—based on penetrance of the mutant phenotype (MATERIALS AND METHODS and Table 2). Only lines with the most penetrant phenotypes were used for complementation tests. This allowed the identification of 17 complementation groups with two or more alleles among 57 lines tested (Table 2). Ten complementation groups were lethal or semilethal, suggesting that the corresponding genes have essential somatic functions and would not have been identified in previous maternal screens (SCHUPBACH and WIESCHAUS 1989, 1991). Due to their shared eggshell phenotype, we named the complementation groups after brands of Cuban cigars. We have determined the genomic location of nine loci by combining SNP mapping with complementation analysis using the 2R deficiency kit (MATERIALS AND METHODS). In this study, we describe the phenotypic characterization of eight of these genes (Table 3).

TABLE 3

Characterization of eight loci on 2R required for DV patterning of the eggshell

		Gurken[a]				Suppression of DV defects[c]	
Classes	Gene	Protein	Localized	Karyosome	C(3)G restriction[b]	*mei-41*	*mei-P22* or *mei-W68*[d]
I	*khc*^{pgs}	+	No	Normal	—	No	—
	bha	+	Yes	Normal	Normal	No	No
	srpk^{cuaba}	+	Yes	Normal	Normal	No	No
II	*nds*	Low	Yes	Normal	Delayed	Yes	No
III	*trin*	+	Yes	Abnormal	Normal	No	No
IV	*dPds5*^{cohiba}	Low	Yes	Abnormal	Delayed	No	Yes
	mtc	Low	Yes	Abnormal	Delayed	No	No
	blv	Low	Yes	Abnormal	Normal	No	No
	spnA[e]	Low	Yes	Abnormal	Delayed	Yes	Yes

[a] Qualitative analysis of Grk production. Protein: +, normal; low, decreased amount detected by fluorescence; localized, correct localization of Grk in stages 6–10.

[b] Timing of restriction of C(3)G to one germ cell in stage 2 egg chambers. Delayed, frequency of C(3)G in more than one cell is >30%; normal, C(3)G always in one cell, $n = 25$.

[c] Frequency of DV polarity defects in eggshells from doubles with *mei-41D*^{3} and with DSB formation mutants ($n > 300$). No, frequency comparable to controls; yes, frequency significantly decreased.

[d] All tests were carried out with DSB formation mutant *mei-P22*^{1}, except for *dPds5*^{cohiba}, which was tested with *mei-W68*^{1}.

[e] Phenotypic characteristics of *dRad51/spnA* for comparison (see Staeva-Vieira *et al.* 2003).

Classification of new DV polarity mutations based on Grk protein distribution and oocyte chromatin condensation: As an initial phenotypic assay, we used oocyte nuclear morphology and Grk protein distribution to characterize the effect of each complementation group on meiosis and oocyte polarity (Gonzalez-Reyes *et al.* 1997) (Figure 2, G–P, and Table 3). By stage 6 of wild-type oogenesis, the DNA within the oocyte nucleus is fully condensed to form a dense karyosome (Figure 2G). At this stage, Grk protein is tightly associated with the oocyte nucleus. Subsequently, at stage 9 of oogenesis, *grk* RNA and protein, together with the oocyte nucleus, move to an anterior corner of the oocyte, where high levels of Grk induce dorsal cell fates in the overlaying follicle cells; at this point, the karyosome takes on a more "relaxed" morphology (Figure 2H) (Neuman-Silberberg and Schupbach 1996). According to our analysis, the new mutants fall into four phenotypic classes. (For a summary of mutant phenotypes and genetic interactions, see Table 3.)

Class I—normal karyosome and Grk protein levels (Figure 2, I–K): Three complementation groups fall into this class (Table 3)—*bahia* (*bha*), *cuaba*, and *partagas* (*pgs*). The two viable *bha* alleles had apparently normal Grk distribution and karyosome morphologies (Figure 2I). This phenotype resembles that of mutations affecting Grk processing or secretion (Valcarcel *et al.* 1999; Bokel *et al.* 2006; Miura *et al.* 2006). In contrast to *bha* mutations, *cuaba* and *pgs* mutants showed defects in egg chamber morphology and oocyte nuclear positioning, respectively (Figure 2, J and K). *cuaba* mutations produced egg chambers with the normal number of germ cells, but the oocyte was abnormally positioned within the oocyte-nurse cell cluster in *cuaba* mutants, not posterior to the nurse cells as in wild type (Figure 2J). This phenotype resembles that caused by DV mutations in genes required for oocyte adhesion to the follicle cells, such as *cadherin*, *dicephalic*, and *brainiac* (Goode *et al.* 1996; Godt and Tepass 1998; Gonzalez-Reyes and St Johnston 1998; McCaffrey *et al.* 2006). We mapped *cuaba* to the coding region *CG8174*, and all four *cuaba* alleles carry mutations in this gene. *CG8174* is predicted to encode the Drosophila homolog of human SR protein kinase 2 (SRPK2). SRPK2 affects alternative splicing of specific RNAs by regulating the function or subcellular localization of SR proteins (Tenenbaum and Aguirre-Ghiso 2005). In *pgs* mutant egg chambers, the oocyte was positioned correctly with respect to the nurse cells. However, at stage 10, when the oocyte nucleus has normally moved to the anterior dorsal side of the oocyte, the oocyte nucleus in *pgs* mutants was found misplaced (Figure 2K). We mapped *pgs* to the genomic region of *kinesin heavy chain* (*khc*), and all *pgs* mutations failed to complement the lethality of a *khc* allele (*khc*^{27}) (Table 2). Since germ-line clones of *khc*^{27} also show a nuclear migration phenotype similar to that of our *pgs* alleles, we conclude that *pgs* mutations affect *khc* (Brendza *et al.* 2002).

Class II—defects in Grk protein synthesis: A single complementation group, *indios* (*nds*), falls into this class. In *nds* mutant egg chambers, Grk protein levels were clearly reduced, although no defects in karyosome morphology were observed (Figure 2L and Table 3). This phenotype resembles that of *grk*, suggesting that *nds* specifically affects the synthesis or stability of *grk* protein or RNA (Gonzalez-Reyes *et al.* 1995; Volpe *et al.* 2001).

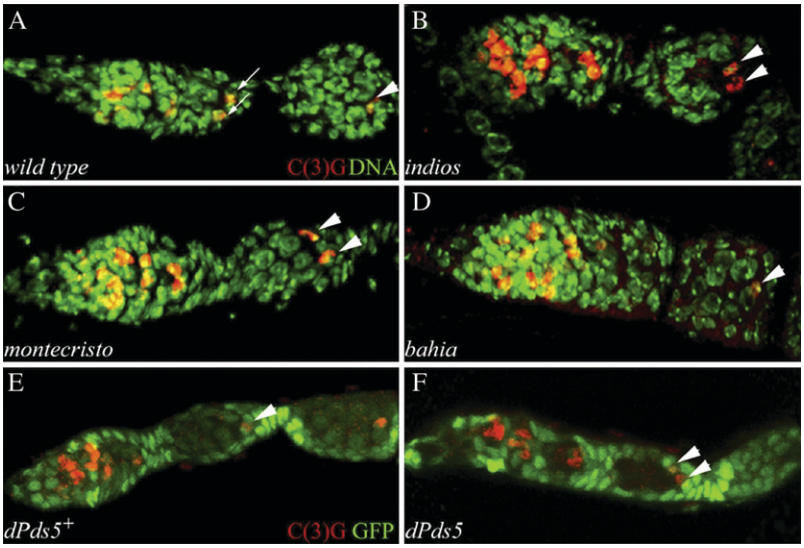

FIGURE 3.—Effect of mutations on the timing of meiotic restriction to the oocyte. (A–D) Localization of the SC protein C(3)G (red) with respect to DNA (green) in meiotic nuclei in germaria (arrows) and stage 2 egg chambers (arrowheads). (A) Control germarium of the genotype *nds*/CyO showing more than one germ cell marked with C(3)G in region 2b and only one marked in the stage 2 chamber. (B) *nds* and (C) *mtc* ovaries showing delays in restriction of C(3)G to the oocyte in stage 2 chambers. (D) *bha* germarium and stage 2 showing normal meiotic restriction of C(3)G ($n > 70$). (E and F) Germ-line clones induced in flies of the genotype FRT 42B $dPds5^{cohiba}$/FRT 42B nls-GFP (green), C(3)G (red). (E) Control germarium and stage 2 with all cells expressing nuclear GFP. (F) $dPds5^{cohiba}$ mutant germ-line clones lack GFP and show delays in C(3)G restriction to stage 2 oocytes (arrowheads).

Class III—defects in karyosome morphology: Seven viable alleles of *trinidad* (*trin*) were identified on the basis of their ventralized and flaccid eggshell phenotype. In these mutant oocytes, chromatin condensation appeared irregular (Figure 2M, inset), while Grk protein levels seemed normal (Figure 2M). It remains unclear how this apparently germ-line-specific gene affects both nuclear morphology and Grk function. A similar phenotype has been observed in mutants defective in actin dynamics such as Src64, Tec29, and Kelch (DODSON *et al.* 1998; DJAGAEVA *et al.* 2005).

Class IV—defects in both Grk production and karyosome formation (Figure 2, N–P): Three complementation groups fall into this class (Table 3)—*bolivar* (*blv*), *montecristo* (*mtc*), and *cohiba*. All three genes seemed to specifically affect karyosome morphology and Grk distribution. These mutants did not alter other aspects of egg chamber development, such as oocyte determination, the number of nurse cells per egg chamber, and the positioning of the oocyte posterior to the nurse cells (data not shown). *blv* and *mtc* oocytes showed a thread-like chromatin morphology typical of other meiotic mutants (Figure 2, N and O, respectively) (GONZALEZ-REYES *et al.* 1997). We used SNP recombination and lack of complementation for female sterility with the *P*-element *PBac{WH}CG15707*^{f06583} to map *mtc* to *CG15707*. All *mtc* alleles carry mutations in this gene, which encodes a 746-aa protein predicted to contain a Tudor domain near its carboxyl terminus (PONTING 1997). BLAST searches using the predicted Mtc protein sequence found significant alignments with a Tudor-domain protein in Anopheles (XM_312463) and several mammalian Tudor-domain proteins. These homologies are, however, restricted to the Tudor domain. In contrast to the karyosome defects observed in *mtc* and *blv*, >50% of *cohiba* karyosomes showed regions of "open" chromatin apparently emerging from a condensed core (Figure 2P, arrow). We mapped *cohiba* by deficiency mapping and complementation analysis with candidate mutants and found that the previously uncharacterized *P*-element *l(2)k13312* failed to complement the lethality of all *cohiba* alleles. Using inverse PCR, we identified the insertion site of *l(2)k13312* upstream of the start codon of *CG17509* (MATERIALS AND METHODS). *CG17509* encodes a Drosophila homolog of the yeast protein Pds5p (CELNIKER *et al.* 2002; DORSETT *et al.* 2005). All *cohiba* alleles carried mutations in the *CG17509* open reading frame, confirming the identity of *cohiba* as Drosophila *Pds5* (*dPds5*). A more detailed description of both *mtc* and $dPds5^{cohiba}$ phenotypes will be presented elsewhere.

Classification of new DV polarity mutations based on restriction of meiosis to the oocyte: To determine whether any of the newly identified DV genes may control meiotic progression, we analyzed the mutants for a block or delay in meiosis. One readout for meiotic progression is the restriction of the synaptonemal complex (SC) component C(3)G to the oocyte in region 3 of the germarium (HUYNH and ST JOHNSTON 2000). In wild type, meiosis initiates in more than one cell per cyst in the germarial region 2 as described in electron micrographs of the SC and by fluorescently labeling C(3)G (CARPENTER 1979; PAGE and HAWLEY 2001). As the cyst matures, the nuclear C(3)G signal restricts from the two pro-oocytes to one cell and synapses are resolved in all nurse cells (Figures 1 and 3, A and E). Mutations in genes controlling RNA and protein transport into the oocyte, such as *egl* and *BicD*, as well as mutations in DSB repair genes such as *spn-A* delay this restriction (HUYNH and ST JOHNSTON 2000; STAEVA-VIEIRA *et al.* 2003; NAVARRO *et al.* 2004).

We assayed the progression of meiosis in the new DV mutants using C(3)G staining (Table 3 and Figure 3). Mutations in three genes, *nds*, *mtc*, and *dPds5*, delayed the restriction of meiosis to the oocyte as evidenced by stage 2 egg chambers that have two C(3)G-positive cells. *nds* mutants showed delays in ~30% of stage 2 egg

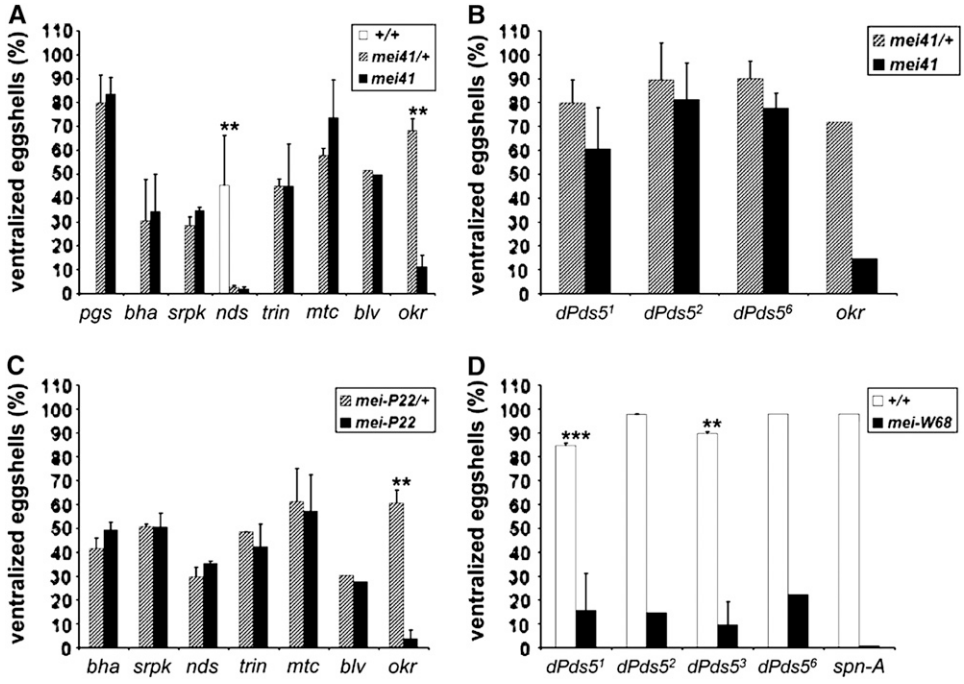

FIGURE 4.—Interactions of mutants with the DSB formation and DNA repair meiotic checkpoint pathways. Frequency of ventralized eggshells produced by mutant flies in an otherwise wild-type (open bars), heterozygous (striped bars) or homozygous mutant (solid bars) background for *mei-41*^{D1} (A and B), *mei-P22*^{1} (C), or *mei-W68*^{1} (D). The error bars, when indicated, give one standard deviation after two independent trials. (A and D) Eggs were derived from *trans*-heterozygous mutant flies for viable allelic combinations (see MATERIALS AND METHODS for the allelic combinations used in each experiment) or homozygous mutant germ-line clones for *khc*^{pgs}. A value for ventralized eggs from individuals of the genotype *nds*^{2}/*nds*^{4}; *mei-41*$^{+}$/*mei-41*$^{+}$ was determined in parallel (open bar in A) to illustrate the dominant genetic interaction (see text). (B and D) Germ-line clones homozygous for *dPds5*^{cohiba} alleles (*dPds5*^{1}, *dPds5*^{2}, *dPds5*^{3}, and *dPds5*^{6}). $^{**}P \leq 0.05$; $^{***}P \leq 0.001$.

chambers ($n = 25$, Figure 3B), *mtc* caused delays in 49% of mutant egg chambers ($n = 25$, Figure 3C), and two *dPds5*^{cohiba} mutant alleles, *dPds5*^{2} and *dPds5*^{6}, showed delays in 29% ($n = 15$) and 40% ($n = 27$) of egg chambers, respectively (Figure 3, E and F). In wild type and egg chambers mutant for *bahia*, *khc*^{pgs}, *srpk*^{cuaba}, *trin*, and *blv*, delays in meiotic restriction were rarely observed (3–5%, Figure 3D).

In summary, mutants in *mtc* and *dPds5* behave like "classical *spindle* mutants" that decrease Grk production, affect karyosome morphology, and delay meiotic restriction. Similar to *vas* mutants, *blv* mutants also affect Grk levels and karyosome morphology but do not show evident delays in meiotic restriction (TOMANCAK *et al.* 1998; HUYNH and ST JOHNSTON 2000). On the other hand, the *nds* phenotype, with decreased Grk protein levels and delayed meiotic restriction but an apparently normal karyosome morphology, and the *trin* phenotype, with normal Grk protein levels, abnormal karyosome condensation, and no evident delays in meiotic restriction, suggest that condensation of meiotic chromatin, timing of meiotic restriction, and control of Grk levels can be uncoupled.

Classification of new DV polarity mutations based on meiotic checkpoint activation and defects in DSB repair: We next determined the genetic relationship of each complementation group with genes affecting DSB repair and meiotic checkpoint activation. As previously shown, mutations in genes controlling checkpoint activation and DSB formation can suppress eggshell ventralization in DSB-repair mutants by restoring Grk protein levels (GHABRIAL and SCHUPBACH 1999; ABDU *et al.* 2002; STAEVA-VIEIRA *et al.* 2003).

We placed mutations of each group in the background of the Drosophila checkpoint protein ATR kinase, *mei-41* (*mei-41*^{D3}), and scored the percentage of ventralized eggshells (see MATERIALS AND METHODS) (LAURENCON *et al.* 2003). Only one group, *nds*, showed significant suppression by *mei-41*^{D3} (Figure 4, A and B, and supplemental Table 1 for *P*-values; http://www.genetics.org/supplemental/). This suppression is dominant since the frequency of DV defects decreased from 45.3% ($n = 546$) in the progeny of *nds* females to 3.1% ($n = 964$) and 2.1% ($n = 828$) in the progeny of *mei-41*^{D3}/+; *indios* and *mei-41*^{D3}; *indios* females, respectively. Interestingly, reducing and eliminating ATR/Mei-41 function in group IV mutants either in germ-line clones homozygous for three lethal *dPds5*^{cohiba} alleles or in combination with viable mutations in *mtc* and *blv* had no significant effect on the frequency of ventralized eggs generated by germ-line clones (Figure 4B).

We subsequently tested the phenotype of our complementation groups in the absence of DSB. This was achieved by combining our mutants with a mutation in either the Spo11p ortholog *mei-W68* or the meiotic chromatin component *mei-P22* (see MATERIALS AND METHODS) (LIU *et al.* 2002; JANG *et al.* 2003). Because the molecular mechanism of *khc*^{pgs} in microtubule-based transport is already established, we excluded this group from the epistatic analysis (Table 3). Mutations from each of the viable complementation groups (*blv*, *bha*, *srpk*^{cuaba}, *nds*, *trin*, and *mtc*) were tested with *mei-P22*^{1}.

However, we did not see suppression of the eggshell phenotype in any of these double mutants (Figure 4C). Since the *dPds5*^{cohiba} alleles are homozygous lethal, we tested *dPds5* in combination with *mei-W68*, which is located on the same chromosome. We induced *mei-W68*^{1} *dPds5*^{cohiba} double mutant homozygous clones using the FRT/ovo^{D} method. In the progeny of these clones, the frequency of ventralized eggshells was significantly reduced (Figure 4D and supplemental Table 1; http://www.genetics.org/supplemental/).

In summary, none of our new mutants behaves identically to mutants in the previously described *spindle* genes *spn-A* and *okr* (Figure 4), which encode enzymes required for DSB repair. Instead, our results suggest that: (1) mutations in *nds* cause Mei-41/ATR checkpoint activation independently of DSB formation; (2) *dPds5* mutants are sensitive to DSBs but seem not to activate the Mei-41/ATR checkpoint; and (3) Blv, Mtc, and Trin may function downstream of, or in parallel to, the Mei-41/ATR checkpoint.

DISCUSSION

In this study, we used a clonal screen to identify genes regulating meiotic progression in Drosophila. Instead of testing directly for defects in meiosis, we used an easy-to-score eggshell phenotype that is produced when the levels or activity of the morphogen Grk are affected. This allowed us to efficiently screen a large number of mutant lines and to identify germ-line-specific genes as well as genes with essential functions. The number of new genes identified is likely less than the total number of 2R genes required for Grk synthesis and function since we discarded mutations that blocked oogenesis (Morris *et al.* 2003). Of the eight genes described in this study, five show meiotic phenotypes. *dPds5*, *nds*, and *mtc* delay meiotic restriction to the oocyte, although only *dPds5* and *nds* genetically interact with *mei-W68* and *mei-41*, respectively. *trin* and *blv* affect the morphology of the karyosome in spite of normal timing in meiotic restriction. This confirms the effectiveness of our screening method for meiotic genes. Genetic and developmental analysis of the newly identified genes provides evidence for new regulatory steps in a network that coordinates Drosophila meiosis and oocyte development.

Chromatin cohesion and DSB formation: One of our complementation groups, *cohiba*, identifies the Drosophila homolog of Pds5p in *Schizosaccharomyces pombe*, Spo76 in *Sordaria macrospore*, and BimD in *Aspergillus nidulans*, which have been found associated with the cohesion complex of mitotic and meiotic chromosomes (van Heemst *et al.* 1999; Panizza *et al.* 2000; Storlazzi *et al.* 2003; Losada *et al.* 2005; Ding *et al.* 2006). More recently, it was shown that depletion of Pds5 affects not only cohesion but also condensation in meiotic prophase (van Heemst *et al.* 1999; Panizza *et al.* 2000; Storlazzi *et al.* 2003; Losada *et al.* 2005; Ding *et al.* 2006). The unique "open chromatin" karyosome defect we observe in *dPds5*^{cohiba} mutants is consistent with a role of Pds5 in chromosome cohesion during Drosophila meiosis. Like Spo76, the *dPds5*^{cohiba} phenotype is suppressed by *Spo11* (*mei-W68*) mutations defective in DSB formation. This suggests that dPds5 is necessary to maintain the structure of the meiotic chromosomes after DSBs are induced (van Heemst *et al.* 1999; Panizza *et al.* 2000; Storlazzi *et al.* 2003; Losada *et al.* 2005; Ding *et al.* 2006). However, in contrast to known DSB repair genes, the meiotic delay and oocyte patterning defects of *dPds*^{cohiba} mutants are not due to activation of ATR/Mei-41-dependent checkpoint. One possibility is that the ATR downstream effector kinase dChk2 is activated via an alternative pathway, such as the Drosophila ataxia-telangiectasia mutated (ATM) homolog, which indeed activates dChk2 in the early embryo independently of ATR (Brodsky *et al.* 2004). Alternatively, *dPds*^{cohiba} mutants may activate a checkpoint that measures cohesion rather than DSB breaks. The only other cohesion protein characterized in Drosophila is the product of the *orientation disruptor* (*ord*). ORD plays a role in early prophase I by maintaining synaptic chromosomes and allowing interhomolog recombination (Webber *et al.* 2004). More importantly and perhaps similar to dPds5, ORD seems not to be required for DSB repair. However, in contrast to *dPds5* mutants, karyosome morphology is normal in *ord* mutants, and an eggshell polarity phenotype has not been reported. Although required for chromatid cohesion, dPds5 and ORD might play complementary roles in SC dynamics: ORD may stabilize the SC in the oocyte, whereas dPds5 may be required for the disassembly of synapses as one of the pro-oocytes regresses from meiosis.

Meiotic restriction to the oocyte: Our screen identified mutations in *montecristo* (*mtc*) that affect the restriction of meiosis to the oocyte. It has been proposed that this delay reflects the activation of the ATR/Mei-41 checkpoint pathway (Huynh and St Johnston 2000). Similar to dPds5, Mtc may control the regression from pachytene in those cyst cells that will not adopt the oocyte fate. The delayed meiotic restriction observed in *mtc* mutants occurs, however, independently of DSB formation or Mei-41 checkpoint activation (Table 3). Mtc contains a Tudor domain. In other Tudor-domain proteins, this domain has been shown to interact with methylated target proteins (Ponting 1997). Identification of specific Mtc targets may clarify its role in meiotic restriction and oocyte patterning.

Karyosome formation and Gurken activity: A particularly intriguing and novel phenotype is uncovered by mutations in *indios* (*nds*). By delaying meiotic restriction and activating Mei-41 without affecting the karyosome morphology, *nds* mutants separate checkpoint activation leading to Grk decrease from checkpoint activation controlling karyosome compaction. The *nds* phenotype also occurs independently of DSBs, suggesting that the

trigger that leads Nds to trigger checkpoint activation is not DNA breaks. The fact that *nds* mutants are extremely sensitive to Mei-41 dosage further suggests that Nds activity may specifically control a branch of the Mei-41 checkpoint regulating Grk activity. In contrast to *nds*, *trin* mutants do not delay meiotic restriction and show defects in the karyosome in spite of normal Grk levels. Like mutants in *src64B* and *tec29*, which show a similar phenotype, Trin may mediate chromatin remodeling in the oocyte by regulating the actin cytoskeleton (Simon *et al.* 1983; Guarnieri *et al.* 1998; Roulier *et al.* 1998; Djagaeva *et al.* 2005). In this context, the DV phenotype of eggs from *trin* mutants may be an indirect effect due to defects in actin cytoskeleton function (Djagaeva *et al.* 2005; Miralles and Visa 2006). The production of collapsed eggs by *trin* mutant germ-line clones is consistent with this idea (Table 2).

Finally, *blv* mutants show striking similarity to *vas* mutants with respect to lack of sensitivity to DSB formation, no evident delays of meiotic restriction, or karyosome and Grk phenotypes (Styhler *et al.* 1998; Tomancak *et al.* 1998; Ghabrial and Schupbach 1999; Huynh and St Johnston 2000). Blv may thus act downstream or independent of the Mei41/ATR checkpoint, and its further characterization may help to understand the effector side of the meiotic checkpoint pathway.

Previous knowledge pointed to Drosophila meiosis as a linear progression of events from homologous chromosome pairing and recombination to meiotic restriction, karyosome formation, and eggshell patterning, with DSB repair as the main checkpoint linking meiosis to Grk signaling. By uncoupling some of these events, our study suggests the existence of a more complex network that links the surveillance of meiotic progression to oocyte patterning.

We thank A. Arkov, Y. Arkova, P. Kunwar, T. Marty, A. Renault, H. Sano, and H. Zinszner for help in performing the mutagenesis screen; and the Lehmann lab for stimulating discussions. We also thank Trudi Schüpbach and Caryn Navarro for scientific advice, and Daria Siekhaus, Lilach Gilboa, and Jessica Seifert for critically reading the manuscript. This work was supported by the Howard Hughes Medical Institute and by Fundação para a Ciência e Tecnologia, Portugal.

LITERATURE CITED

Abdu, U., M. Brodsky and T. Schupbach, 2002 Activation of a meiotic checkpoint during Drosophila oogenesis regulates the translation of Gurken through Chk2/Mnk. Curr. Biol. **12:** 1645–1651.

Abdu, U., D. Bar and T. Schupbach, 2006 spn-F encodes a novel protein that affects oocyte patterning and bristle morphology in Drosophila. Development **133:** 1477–1484.

Ashburner, M., 1989 *Drosophila: A Laboratory Manual.* Cold Spring Harbor Laboratory Press, Cold Spring Harbor, NY.

Berger, J., T. Suzuki, K. A. Senti, J. Stubbs, G. Schaffner *et al.*, 2001 Genetic mapping with SNP markers in Drosophila. Nat. Genet. **29:** 475–481.

Bhalla, N., and A. F. Dernburg, 2005 A conserved checkpoint monitors meiotic chromosome synapsis in Caenorhabditis elegans. Science **310:** 1683–1686.

Bokel, C., S. Dass, M. Wilsch-Brauninger and S. Roth, 2006 Drosophila Cornichon acts as cargo receptor for ER export of the TGF{alpha}-like growth factor Gurken. Development **133:** 459–470.

Brendza, R. P., L. R. Serbus, J. B. Duffy and W. M. Saxton, 2000 A function for kinesin I in the posterior transport of oskar mRNA and Staufen protein. Science **289:** 2120–2122.

Brendza, R. P., L. R. Serbus, W. M. Saxton and J. B. Duffy, 2002 Posterior localization of dynein and dorsal-ventral axis formation depend on kinesin in Drosophila oocytes. Curr. Biol. **12:** 1541–1545.

Brodsky, M. H., B. T. Weinert, G. Tsang, Y. S. Rong, N. M. McGinnis *et al.*, 2004 Drosophila melanogaster MNK/Chk2 and p53 regulate multiple DNA repair and apoptotic pathways following DNA damage. Mol. Cell Biol. **24:** 1219–1231.

Carpenter, A. T., 1979 Synaptonemal complex and recombination nodules in wild-type *Drosophila melanogaster* females. Genetics **92:** 511–541.

Celniker, S. E., D. A. Wheeler, B. Kronmiller, J. W. Carlson, A. Halpern *et al.*, 2002 Finishing a whole-genome shotgun: release 3 of the Drosophila melanogaster euchromatic genome sequence. Genome Biol. **3:** RESEARCH0079.

Chou, T. B., and N. Perrimon, 1992 Use of a yeast site-specific recombinase to produce female germline chimeras in Drosophila. Genetics **131:** 643–653.

de Cuevas, M., M. A. Lilly and A. C. Spradling, 1997 Germline cyst formation in Drosophila. Annu. Rev. Genet. **31:** 405–428.

Ding, D. Q., N. Sakurai, Y. Katou, T. Itoh, K. Shirahige *et al.*, 2006 Meiotic cohesins modulate chromosome compaction during meiotic prophase in fission yeast. J. Cell Biol. **174:** 499–508.

Djagaeva, I., S. Doronkin and S. K. Beckendorf, 2005 Src64 is involved in fusome development and karyosome formation during Drosophila oogenesis. Dev. Biol. **284:** 143–156.

Dodson, G. S., D. J. Guarnieri and M. A. Simon, 1998 Src64 is required for ovarian ring canal morphogenesis during Drosophila oogenesis. Development **125:** 2883–2892.

Dorsett, D., J. C. Eissenberg, Z. Misulovin, A. Martens, B. Redding *et al.*, 2005 Effects of sister chromatid cohesion proteins on cut gene expression during wing development in Drosophila. Development **132:** 4743–4753.

Findley, S. D., M. Tamanaha, N. J. Clegg and H. Ruohola-Baker, 2003 Maelstrom, a Drosophila spindle-class gene, encodes a protein that colocalizes with Vasa and RDE1/AGO1 homolog, Aubergine, in nuage. Development **130:** 859–871.

Ghabrial, A., and T. Schupbach, 1999 Activation of a meiotic checkpoint regulates translation of Gurken during Drosophila oogenesis. Nat. Cell Biol. **1:** 354–357.

Ghabrial, A., R. P. Ray and T. Schupbach, 1998 okra and spindle-B encode components of the RAD52 DNA repair pathway and affect meiosis and patterning in Drosophila oogenesis. Genes Dev. **12:** 2711–2723.

Ghiglione, C., E. A. Bach, Y. Paraiso, K. L. Carraway, III, S. Noselli *et al.*, 2002 Mechanism of activation of the Drosophila EGF Receptor by the TGFalpha ligand Gurken during oogenesis. Development **129:** 175–186.

Godt, D., and U. Tepass, 1998 Drosophila oocyte localization is mediated by differential cadherin-based adhesion. Nature **395:** 387–391.

Gonzalez-Reyes, A., and D. St Johnston, 1998 The Drosophila AP axis is polarised by the cadherin-mediated positioning of the oocyte. Development **125:** 3635–3644.

Gonzalez-Reyes, A., H. Elliott and D. St Johnston, 1995 Polarization of both major body axes in Drosophila by gurken-torpedo signalling. Nature **375:** 654–658.

Gonzalez-Reyes, A., H. Elliot and D. St Johnston, 1997 Oocyte determination and the origin of polarity in Drosophila: the role of the spindle genes. Development **124:** 4927–4937.

Goode, S., M. Morgan, Y. P. Liang and A. P. Mahowald, 1996 Brainiac encodes a novel, putative secreted protein that cooperates with Grk TGF alpha in the genesis of the follicular epithelium. Dev. Biol. **178:** 35–50.

Guarnieri, D. J., G. S. Dodson and M. A. Simon, 1998 SRC64 regulates the localization of a Tec-family kinase required for Drosophila ring canal growth. Mol. Cell. **1:** 831–840.

Huynh, J. R., and D. St Johnston, 2000 The role of BicD, Egl, Orb and the microtubules in the restriction of meiosis to the Drosophila oocyte. Development **127:** 2785–2794.

Jang, J. K., D. E. Sherizen, R. Bhagat, E. A. Manheim and K. S. McKim, 2003 Relationship of DNA double-strand breaks to synapsis in Drosophila. J. Cell Sci. **116:** 3069–3077.

Kennerdell, J. R., S. Yamaguchi and R. W. Carthew, 2002 RNAi is activated during Drosophila oocyte maturation in a manner dependent on aubergine and spindle-E. Genes Dev. **16:** 1884–1889.

Kuzminov, A., 2001 DNA replication meets genetic exchange: chromosomal damage and its repair by homologous recombination. Proc. Natl. Acad. Sci. USA **98:** 8461–8468.

Laurencon, A., A. Purdy, J. Sekelsky, R. S. Hawley and T. T. Su, 2003 Phenotypic analysis of separation-of-function alleles of MEI-41, Drosophila ATM/ATR. Genetics **164:** 589–601.

Liu, H., J. K. Jang, N. Kato and K. S. McKim, 2002 mei-P22 encodes a chromosome-associated protein required for the initiation of meiotic recombination in *Drosophila melanogaster*. Genetics **162:** 245–258.

Losada, A., T. Yokochi and T. Hirano, 2005 Functional contribution of Pds5 to cohesin-mediated cohesion in human cells and Xenopus egg extracts. J. Cell Sci. **118:** 2133–2141.

McCaffrey, R., D. St Johnston and A. Gonzalez-Reyes, 2006 A novel mutant phenotype implicates dicephalic in cyst formation in the Drosophila ovary. Dev. Dyn. **235:** 908–917.

Miralles, F., and N. Visa, 2006 Actin in transcription and transcription regulation. Curr. Opin. Cell Biol. **18:** 261–266.

Miura, G. I., J. Buglino, D. Alvarado, M. A. Lemmon, M. D. Resh *et al.*, 2006 Palmitoylation of the EGFR ligand Spitz by Rasp increases Spitz activity by restricting its diffusion. Dev. Cell **10:** 167–176.

Moore, L. A., H. T. Broihier, M. Van Doren, L. B. Lunsford and R. Lehmann, 1998 Identification of genes controlling germ cell migration and embryonic gonad formation in Drosophila. Development **125:** 667–678.

Morris, J., and R. Lehmann, 1999 Drosophila oogenesis: versatile spn doctors. Curr. Biol. **9:** R55–58.

Morris, J. Z., C. Navarro and R. Lehmann, 2003 Identification and analysis of mutations in bob, Doa and eight new genes required for oocyte specification and development in *Drosophila melanogaster*. Genetics **164:** 1435–1446.

Navarro, C., H. Puthalakath, J. M. Adams, A. Strasser and R. Lehmann, 2004 Egalitarian binds dynein light chain to establish oocyte polarity and maintain oocyte fate. Nat. Cell Biol. **6:** 427–435.

Neuman-Silberberg, F. S., and T. Schupbach, 1994 Dorsoventral axis formation in Drosophila depends on the correct dosage of the gene gurken. Development **120:** 2457–2463.

Neuman-Silberberg, F. S., and T. Schupbach, 1996 The Drosophila TGF-alpha-like protein Gurken: expression and cellular localization during Drosophila oogenesis. Mech. Dev. **59:** 105–113.

Page, S. L., and R. S. Hawley, 2001 c(3)G encodes a Drosophila synaptonemal complex protein. Genes Dev. **15:** 1330–1343.

Page, S. L., and R. S. Hawley, 2004 The genetics and molecular biology of the synaptonemal complex. Annu. Rev. Cell Dev. Biol. **20:** 525–558.

Panizza, S., T. Tanaka, A. Hochwagen, F. Eisenhaber and K. Nasmyth, 2000 Pds5 cooperates with cohesin in maintaining sister chromatid cohesion. Curr. Biol. **10:** 1557–1564.

Ponting, C. P., 1997 Tudor domains in proteins that interact with RNA. Trends Biochem. Sci. **22:** 51–52.

Queenan, A. M., G. Barcelo, C. Van Buskirk and T. Schupbach, 1999 The transmembrane region of Gurken is not required for biological activity, but is necessary for transport to the oocyte membrane in Drosophila. Mech. Dev. **89:** 35–42.

Roeder, G. S., and J. M. Bailis, 2000 The pachytene checkpoint. Trends Genet. **16:** 395–403.

Roulier, E. M., S. Panzer and S. K. Beckendorf, 1998 The Tec29 tyrosine kinase is required during Drosophila embryogenesis and interacts with Src64 in ring canal development. Mol. Cell **1:** 819–829.

Saunders, C., and R. S. Cohen, 1999 The role of oocyte transcription, the 5′UTR, and translation repression and derepression in Drosophila gurken mRNA and protein localization. Mol. Cell. **3:** 43–54.

Schupbach, T., and E. Wieschaus, 1989 Female sterile mutations on the second chromosome of *Drosophila melanogaster*. I. Maternal effect mutations. Genetics **121:** 101–117.

Schupbach, T., and E. Wieschaus, 1991 Female sterile mutations on the second chromosome of *Drosophila melanogaster*. II. Mutations blocking oogenesis or altering egg morphology. Genetics **129:** 1119–1136.

Simon, M. A., T. B. Kornberg and J. M. Bishop, 1983 Three loci related to the src oncogene and tyrosine-specific protein kinase activity in Drosophila. Nature **302:** 837–839.

Spradling, A. C., 1993 Developmental genetics of oogenesis, pp. 1–70 in *Drosophila Development*, edited by M. Bate and A. Martinez-Arias. Cold Spring Harbor Laboratory Press, Cold Spring Harbor, NY.

Staeva-Vieira, E., S. Yoo and R. Lehmann, 2003 An essential role of DmRad51/SpnA in DNA repair and meiotic checkpoint control. EMBO J. **22:** 5863–5874.

Storlazzi, A., S. Tesse, S. Gargano, F. James, N. Kleckner *et al.*, 2003 Meiotic double-strand breaks at the interface of chromosome movement, chromosome remodeling, and reductional division. Genes Dev. **17:** 2675–2687.

Styhler, S., A. Nakamura, A. Swan, B. Suter and P. Lasko, 1998 vasa is required for GURKEN accumulation in the oocyte, and is involved in oocyte differentiation and germline cyst development. Development **125:** 1569–1578.

Swan, A., and B. Suter, 1996 Role of Bicaudal-D in patterning the Drosophila egg chamber in mid-oogenesis. Development **122:** 3577–3586.

Swan, A., T. Nguyen and B. Suter, 1999 Drosophila Lissencephaly-1 functions with Bic-D and dynein in oocyte determination and nuclear positioning. Nat. Cell Biol. **1:** 444–449.

Tenenbaum, S. A., and J. Aguirre-Ghiso, 2005 Dephosphorylation shows SR proteins the way out. Mol. Cell **20:** 499–501.

Tomancak, P., A. Guichet, P. Zavorszky and A. Ephrussi, 1998 Oocyte polarity depends on regulation of gurken by Vasa. Development **125:** 1723–1732.

Valcarcel, R., U. Weber, D. B. Jackson, V. Benes, W. Ansorge *et al.*, 1999 Sec61beta, a subunit of the protein translocation channel, is required during Drosophila development. J. Cell Sci. **112**(Pt 23): 4389–4396.

van Heemst, D., F. James, S. Poggeler, V. Berteaux-Lecellier and D. Zickler, 1999 Spo76p is a conserved chromosome morphogenesis protein that links the mitotic and meiotic programs. Cell **98:** 261–271.

Volpe, A. M., H. Horowitz, C. M. Grafer, S. M. Jackson and C. A. Berg, 2001 *Drosophila rhino* encodes a female-specific chromodomain protein that affects chromosome structure and egg polarity. Genetics **159:** 1117–1134.

Webber, H. A., L. Howard and S. E. Bickel, 2004 The cohesion protein ORD is required for homologue bias during meiotic recombination. J. Cell Biol. **164:** 819–829.

Wilhelm, J. E., M. Buszczak and S. Sayles, 2005 Efficient protein trafficking requires trailer hitch, a component of a ribonucleoprotein complex localized to the ER in Drosophila. Dev. Cell **9:** 675–685.

Yohn, C. B., L. Pusateri, V. Barbosa and R. Lehmann, 2003 l(3)-malignant brain tumor and three novel genes are required for Drosophila germ-cell formation. Genetics **165:** 1889–1900.

Communicating editor: T. C. Kaufman